

Upper limits on DM annihilation cross sections from the first AMS-02 antiproton data

Hong-Bo Jin^{a,b}, Yue-Liang Wu^{a,c,d}, and Yu-Feng Zhou^{a,c} *

^{a)} *State Key Laboratory of Theoretical Physics, ^{b)} National Astronomical Observatories, Chinese Academy of Sciences,*

^{c)} *Kavli Institute for Theoretical Physics China, Institute of Theoretical Physics Chinese Academy of Sciences,*

^{d)} *University of Chinese Academy of Sciences, Beijing, 100190, P.R. China*

March 2, 2024

Abstract

The first measurement on the antiproton to proton ratio by the AMS-02 collaboration agrees with the expectation from conventional cosmic-ray secondaries in the kinetic energy range $\sim 20 - 100$ GeV, which can be turned into stringent upper limits on the annihilation cross sections of dark matter (DM) above ~ 300 GeV. Using the GALPROP code, we derive the upper limits in various propagation models and DM profiles. We show that in the “conventional” propagation model, for the $q\bar{q}$, $b\bar{b}$, and W^+W^- final states, the constraints could be more stringent than that derived from the recent Fermi-LAT gamma-ray data on the dwarf spheroidal satellite galaxies. Making use of the typical minimal, median and maximal models obtained from a previous GALPROP based global fit to the preliminary AMS-02 data, we show that the variation of the upper limits is about a factor of five. The possibility of DM contributions to the low and very high energy \bar{p}/p data is discussed.

*Emails: hbjin@bao.ac.cn, ylwu@itp.ac.cn, yfzhou@itp.ac.cn

Dark matter (DM) is known to contribute to 26.8% of the total energy density of the Universe [1]. However, its particle nature remains largely unknown. If the DM particles can annihilate or decay into the standard model (SM) final states, they will contribute to new primary sources of cosmic-ray particles, and result in significant changes in the spectra of the cosmic-ray antiparticles such as positrons and antiprotons, as these species are assumed to be secondaries in the conventional cosmic-ray propagation theory. Antiprotons are highly expected from DM annihilation in many DM models, and unlikely to be generated from the nearby pulsars. Compared with cosmic-ray electrons/positrons, the cosmic-ray antiprotons lose much less energy during propagation, and can travel through longer distance in the Galaxy, which makes the antiproton flux more sensitive to the uncertainties in the propagation parameters and the DM profiles.

Recently, the AMS-02 collaboration has released the first preliminary result of the cosmic-ray antiproton to proton flux ratio \bar{p}/p [2]. The measured kinetic energies of the antiprotons have been extended to ~ 450 GeV. Although the spectrum of \bar{p}/p at high energies above 100 GeV tend to be relatively flat, within uncertainties the AMS-02 data are consistent with the background of secondary antiprotons, which can be used to set stringent upper limits on the dark matter (DM) annihilation cross sections, especially for high mass DM particles. The constraints on the DM properties from antiprotons have been investigated previously before AMS-02 (see e.g. [3, 4, 5, 6, 7]). In this work, we explore the significance of the new AMS-02 \bar{p}/p data on constraining the annihilation cross sections of the DM particles in various propagation models and DM profiles. Four representative background models are considered with four different DM profiles. We derive the upper limits using the GALPROP code and show that in the “conventional” propagation model with Einasto DM profile, the constraints could be more stringent than that derived from the Fermi-LAT gamma-ray data on the dwarf spheroidal satellite galaxies. Making use of the typical minimal, median and maximal models obtained from a previous GALPROP based global fit to the preliminary AMS-02 data, we show that the uncertainties on the upper limits is around a factor of five.

We start with a brief overview on the main features of the cosmic-ray propagation within the Galaxy. The Galactic halo within which the diffusion processes occur is parametrized by a cylinder with radius $R_h = 20$ kpc and half-height $Z_h = 1 - 20$ kpc. The diffusion equation for the cosmic-ray charged particles reads (see e.g. [8])

$$\begin{aligned} \frac{\partial \psi}{\partial t} = & \nabla(D_{xx}\nabla\psi - \mathbf{V}_c\psi) + \frac{\partial}{\partial p}p^2D_{pp}\frac{\partial}{\partial p}\frac{1}{p^2}\psi - \frac{\partial}{\partial p}\left[\dot{p}\psi - \frac{p}{3}(\nabla \cdot \mathbf{V}_c)\psi\right] \\ & - \frac{1}{\tau_f}\psi - \frac{1}{\tau_r}\psi + q(\mathbf{r}, p), \end{aligned} \quad (1)$$

where $\psi(\mathbf{r}, p, t)$ is the number density per unit of total particle momentum. For steady-

state diffusion, it is assumed that $\partial\psi/\partial t = 0$. The number densities of cosmic-ray particles are vanishing at the boundary of the halo, i.e., $\psi(R_h, z, p) = \psi(R, \pm Z_h, p) = 0$. The energy dependent spatial diffusion coefficient D_{xx} is parametrized as $D_{xx} = \beta D_0 (\rho/\rho_0)^\delta$, where $\rho = p/(Ze)$ is the rigidity of the cosmic-ray particle with electric charge Ze . The power spectral index δ can have different values $\delta = \delta_{1(2)}$ when ρ is below (above) a reference rigidity ρ_0 . The coefficient D_0 is a normalization constant, and $\beta = v/c$ is the velocity of the cosmic-ray particle. The convection term in the diffusion equation is related to the drift of cosmic-ray particles from the Galactic disc due to the Galactic wind. The diffusion in momentum space is described by the reacceleration parameter D_{pp} which is related to the velocity of disturbances in the hydrodynamical plasma, and described by the Alfvén speed V_a [8]. In Eq. (1), the momentum loss rate is denoted by \dot{p} which could be due to ionization in the interstellar medium neutral matter, Coulomb scattering off thermal electrons in ionized plasma, bremsstrahlung, synchrotron radiation, and inverse Compton scattering, etc.. The parameter $\tau_f(\tau_r)$ is the time scale for fragmentation (radioactive decay) of the cosmic-ray nuclei as they interact with interstellar hydrogen and helium.

The spectrum of a primary source term for a cosmic-ray nucleus A is assumed to have a broken power law behaviour $dq_A(p)/dp \propto (\rho/\rho_{As})^{\gamma_A}$ with $\gamma_A = \gamma_{A1}(\gamma_{A2})$ for the nucleus rigidity ρ below (above) a reference rigidity ρ_{As} . The spatial distribution of the primary sources is taken from Ref. [9]. Secondary antiprotons are created dominantly from inelastic pp - and pA -collisions with the interstellar gas. The corresponding source term reads

$$q(p) = \beta c n_i \sum_{i=\text{H,He}} \int dp' \frac{\sigma_i(p, p')}{dp'} n_p(p') \quad (2)$$

where n_i is the number density of the interstellar hydrogen (helium), n_p is the number density of primary cosmic-ray proton per total momentum, and $d\sigma_i(p, p')/dp'$ is the differential cross section for $p + \text{H(He)} \rightarrow \bar{p} + X$. In calculating the antiprotons, inelastic scattering to produce “tertiary” antiprotons should be taken into account.

The primary source term from the annihilation of Majorana DM particles has the following form

$$q(\mathbf{r}, p) = \frac{\rho(\mathbf{r})^2}{2m_\chi^2} \langle \sigma v \rangle \sum_X \eta_X \frac{dN^{(X)}}{dp}, \quad (3)$$

where $\langle \sigma v \rangle$ is the velocity-averaged DM annihilation cross section multiplied by DM relative velocity (referred to as cross section). $\rho(\mathbf{r})$ is the DM energy density distribution function, and $dN^{(X)}/dp$ is the injection energy spectrum of antiprotons from DM annihilating into SM final states through all possible intermediate states X with η_X the corresponding branching fractions.

The interstellar flux of the cosmic-ray particle is related to its density function as $\Phi = v\psi(\mathbf{r}, p)/(4\pi)$. At the top of the atmosphere (TOA) of the Earth, the fluxes of

cosmic-rays are affected by solar winds and the heliospheric magnetic field. This effect is taken into account using the force-field approximation which involves a parameter ϕ , the so called Fisk potential [10]. In this work, we shall take $\phi = 550$ MV in the numerical analysis.

We shall solve the diffusion equation of Eq. (1) using the publicly available code GALPROP v54 [11, 12, 13, 14, 15] which utilizes realistic astronomical information on the distribution of interstellar gas and other data as input, and considers various kinds of observables in a self-consistent way. Other approaches based on simplified assumptions on the Galactic gas distribution which allow for fast analytic solutions can be found in Refs. [16,].

We first consider the so-called “conventional” diffusive re-acceleration (DR) model [13, 15] which is commonly adopted by the current experimental collaborations such as PAMELA [21, 22, 23] and Fermi-LAT [24, 25] as a benchmark model for the astrophysical backgrounds. It is useful to consider this model as a reference model to understand how the DM properties could be constrained by the AMS-02 data. Then we consider three representative propagation models selected from a large sample of models obtained from a global Bayesian MCMC fit to the preliminary AMS-02 proton and B/C data using the GALPROP code [26]. They are selected to represent the typically minimal (MIN), median (MED) and maximal (MAX) antiproton fluxes within 95% CL, corresponding to the region enveloping 95% of the MCMC samples with highest likelihoods in a six-dimensional parameter space. For simple Gaussian posterior distributions, it corresponds to $\Delta\chi^2 = 12.59$ for six degrees of freedom. The parameters in the four models are summarized in Tab. 1.

Note that the “MIN”, “MED” and “MAX” models used in this work are different from and complementary to that given in Ref. [27] in several ways: i) they are obtained using the fully numerical GALPROP code which is consistent with the analysis framework of this work while that in Ref. [27] are based on the two-zone diffusion model with the assumption of simplified galactic geometry and uniform interstellar gas distributions. ii) they correspond to the DR propagation model while that in Ref. [27] the models with diffusive-reacceleration plus a constant convection velocity V_c are considered. In the GALPROP approach, it is known that the spectral shape of the B/C flux ratio is better reproduced without including the convection term; iii) the models in this work are based on the global fit to the preliminary AMS-02 data of proton flux and B/C flux ratio, while the models in Ref. [27] are based on the much older HEAO-3 data on B/C ratio with significantly lower precision. Consequently, the uncertainties in the prediction for the DM induced antiproton fluxes are much larger; iv) the Bayesian analysis was used in deriving these models, while in Ref. [27] the authors performed a frequentist analysis. The credible intervals obtained from the Bayesian analysis can be different from that using the

confidence levels based on a given value of $\Delta\chi^2$.

The predicted proton flux and the B/C flux ratio in these models are shown in Fig. 1, together with the latest AMS-02 data [2]. The figures show an overall agreement with the current data in these models. In the “conventional” model, the predicted B/C ratio is a little higher for the kinetic energy below ~ 10 GeV/n, but are consistent with the B/C data in the higher energies. Note that the theoretical predictions from Ref. [26] is based on the analysis of the previous preliminary AMS-02 results announced at the conference ICRC(2013) [28, 29]. So far the AMS-02 data on the B/C flux ratio is still unpublished. We will update the whole analysis in Ref. [26] after they get published, in a future work. The predictions for the background of the \bar{p}/p flux ratio in these models are shown in Fig. 2. The “MIN”, “MED” and “MAX” models are highly degenerate in the background \bar{p}/p ratio. Compared with these models, the “conventional” model predicts more low energy antiprotons but at high energies above ~ 500 GeV, the predicted antiprotons are much less. In all the four DR propagation models, below ~ 10 GeV the GALPROP based calculations underpredict the \bar{p}/p flux ratio by $\sim 40\%$, which is a known issue. The agreement with the low energy \bar{p} data can be improved by introducing breaks in diffusion coefficients [30], “fresh” nuclei component [31] or a DM contribution [3]. Note that at energies below ~ 10 GeV, the uncertainties due to the solar modulation and the propagation parameters increase significantly. The predictions for low energy \bar{p}/p ratio can be easily modified by introducing an independent Fisk potential ϕ for \bar{p} and an energy-dependent overall normalization factor as discussed in Ref.[32]. In this work, we instead use these DR models to derived very conservative upper limits on the annihilation cross sections of light DM particles. Note however that in the DR propagation models, the background predictions agree with the AMS-02 data well at higher energies $\sim 10 - 100$ GeV, which can be turned into stringent constraints on the nature of heavy DM particles.

| model | $R(\text{kpc})$ | $Z_h(\text{kpc})$ | D_0 | ρ_0 | δ_1/δ_2 | $V_a(\text{km/s})$ | ρ_s | γ_{p1}/γ_{p2} |
|--------------|-----------------|-------------------|-------|----------|---------------------|--------------------|----------|---------------------------|
| Conventional | 20 | 4.0 | 5.75 | 4.0 | 0.34/0.34 | 36.0 | 9.0 | 1.82/2.36 |
| MIN | 20 | 1.8 | 3.53 | 4.0 | 0.3/0.3 | 42.7 | 10.0 | 1.75/2.44 |
| MED | 20 | 3.2 | 6.50 | 4.0 | 0.29/0.29 | 44.8 | 10.0 | 1.79/2.45 |
| MAX | 20 | 6.0 | 10.6 | 4.0 | 0.29/0.29 | 43.4 | 10.0 | 1.81/2.46 |

TAB. 1: Parameters in the propagation models “Conventional” [13, 15], “MIN”, “MED” and “MAX” models from Ref. [26]. D_0 is in units of $10^{28}\text{cm}^2 \cdot \text{s}^{-1}$, the break rigidities ρ_0 and ρ_s are in units of GV.

The flux cosmic-ray antiprotons from DM annihilation depend also significantly on the

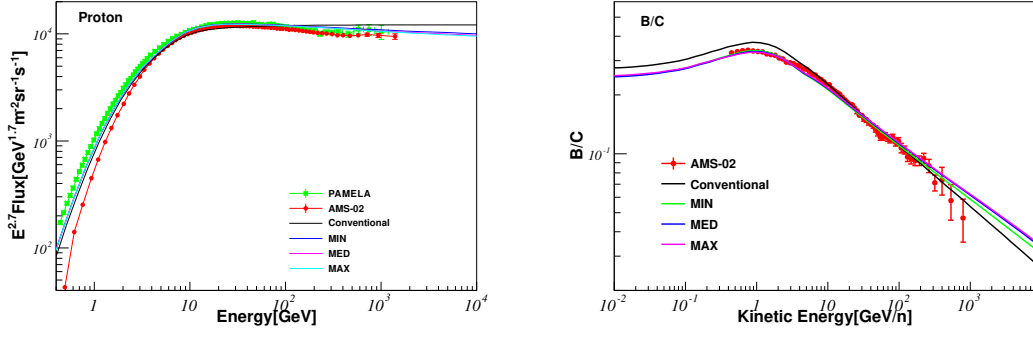


FIG. 1: Predictions for the proton flux (left) and the B/C flux ratio (right) in the four propagation models listed in Tab. 1. The latest data of proton flux from AMS-02 [2] and PAMELA [33, 34] are shown.

choice of DM halo profile. N-body simulations suggest a universal form of the DM profile

$$\rho(r) = \rho_{\odot} \left(\frac{r}{r_{\odot}} \right)^{-\gamma} \left(\frac{1 + (r_{\odot}/r_s)^{\alpha}}{1 + (r/r_{\odot})^{\alpha}} \right)^{(\beta-\gamma)/\alpha}, \quad (4)$$

where $\rho_{\odot} \approx 0.43 \text{ GeV cm}^{-3}$ is the local DM energy density [35]. The values of the parameters α , β , γ and r_s for the Navarfro-Frenk-White (NFW) profile [36], the isothermal profile [37] and the Moore profile [38, 39] are summarized in Tab. 2. An other widely

| | α | β | γ | $r_s(\text{kpc})$ |
|------------|----------|---------|----------|-------------------|
| NFW | 1.0 | 3.0 | 1.0 | 20 |
| Isothermal | 2.0 | 2.0 | 0 | 3.5 |
| Moore | 1.5 | 3.0 | 1.5 | 28.0 |

TAB. 2: Values of parameters α , β , γ and r_s for three DM halo models, NFW [36], Isothermal [37], and Moore [38, 39].

adopted DM profile is the Einasto profile [40]

$$\rho(r) = \rho_{\odot} \exp \left[- \left(\frac{2}{\alpha_E} \right) \left(\frac{r^{\alpha_E} - r_{\odot}^{\alpha_E}}{r_s^{\alpha_E}} \right) \right], \quad (5)$$

with $\alpha_E \approx 0.17$ and $r_s \approx 20 \text{ kpc}$.

We consider three reference DM annihilation channels $\bar{\chi}\chi \rightarrow XX$ where $XX = q\bar{q}$, $b\bar{b}$ and W^+W^- . The energy spectra of these channels are similar at high energies. The main difference is in the average number of total antiprotons N_X per DM annihilation of each

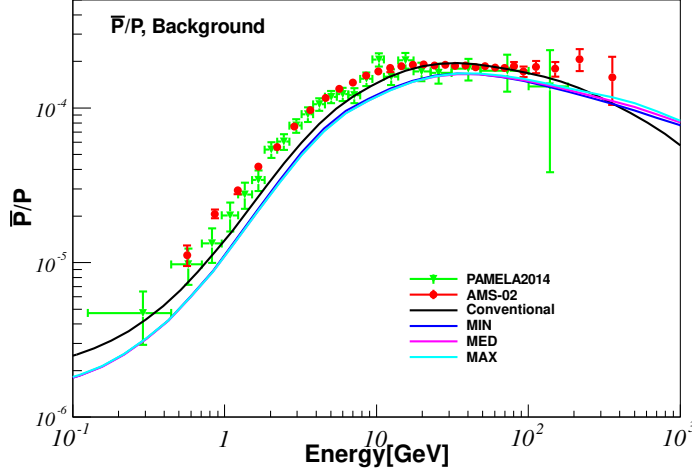


FIG. 2: Predictions for the \bar{p}/p ratio from the four propagation models list in Tab. 1. The data from AMS-02 [2] and PAMELA [33] are shown.

channel. For a DM particle mass $m_\chi = 500$ GeV, the values of N_X for typical final states are $N_{q\bar{q}} = 2.97$ ($q = u, d$), $N_{b\bar{b}} = 2.66$, and $N_{WW} = 1.42$. The injection spectra $dN^{(X)}/dp$ from DM annihilation are calculated using the numerical package PYTHIA v8.175 [41], in which the long-lived particles such as neutron and K_L are allowed to decay and the final state interaction are taken into account. Since PYTHIA v8.15 the polarization and correlation of final states in τ -decays has been taken into account [42].

In this work, we shall first derive the upper limits on the DM annihilation cross section as a function of DM particle mass, using the frequentist χ^2 -analyses. The expression of χ^2 is defined as

$$\chi^2 = \sum_i \frac{(f_i^{\text{th}} - f_i^{\text{exp}})^2}{\sigma_i^2}, \quad (6)$$

where f_i^{th} are the theoretical predictions. f_i^{exp} and σ_i are the central values and errors of experimental data, respectively. The index i runs over all the available data points. For a given DM particle mass, we first calculate the minimal value χ^2_{min} of the χ^2 -function, and then derive the one-side 95% CL upper limits on the annihilation cross section, corresponding to $\Delta\chi^2 = 3.84$ for one parameter. All of the 30 data points of the AMS-02 \bar{p}/p data are included in calculating the limits.

In Fig. 3, we show the obtained upper limits on the cross sections for DM particle annihilation into $b\bar{b}$ final states from the AMS-02 \bar{p}/p data in the “conventional”, “MED”, “MIN” and “MAX” propagation models. Four different DM profiles NFW [36], Isothermal [37], Einasto [40] and Moore [38, 39] are considered. As can be seen, the upper limits

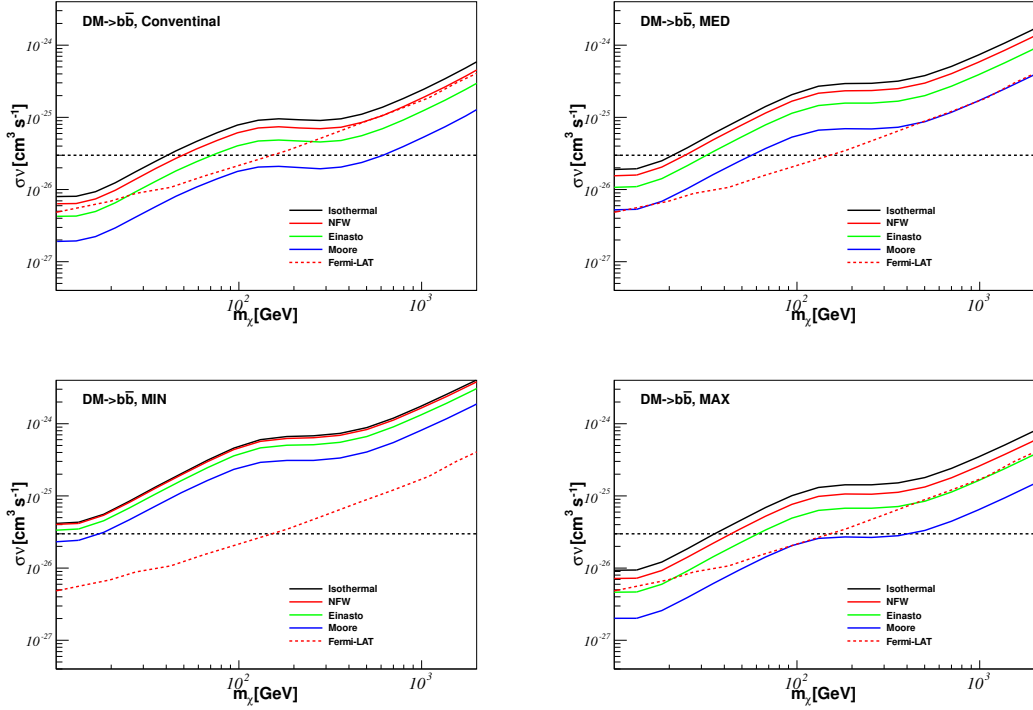


FIG. 3: Upper limits on the cross sections for DM particle annihilation into $b\bar{b}$ final states from the AMS-02 \bar{p}/p data in the “conventional” (upper left), “MED” (upper right), “MIN” (lower left) and “MAX” (lower right) propagation models. Four DM profiles NFW [36], Isothermal [37], Einasto [40] and Moore [38, 39] are considered. The upper limits from the Fermi-LAT 6-year gamma-ray data of the dwarf spheroidal satellite galaxies of the Milky Way are also shown [43]. The horizontal line indicates the typical thermal annihilation cross section $\langle\sigma v\rangle = 3 \times 10^{-26} \text{cm}^3 \text{s}^{-1}$.

as a function of m_χ show some smooth structure for all the final states and DM profiles. The limits tend to be relatively stronger at $m_\chi \approx 300$ GeV, which is related to the fact that the background predictions agree with the data well at the antiproton energy range $\sim 20 - 100$ GeV. For a comparison, the upper limits from the Fermi-LAT 6-year gamma-ray data of the dwarf spheroidal satellite galaxies of the Milky Way are also shown [43]. In the “conventional” model, the upper limits from the AMS-02 \bar{p}/p data are found to be compatible with that derived from the Fermi-LAT gamma-ray data for $m_\chi \gtrsim 300$ GeV. This observation holds for most of the DM profiles. In the “MED” model, the constraints are relatively weaker, which is related to the under prediction of low energy antiprotons in this model and the limits are more conservative. For an estimation of the uncertainties due to the propagation models, from the “MIN” model to the “MAX” model, we find that

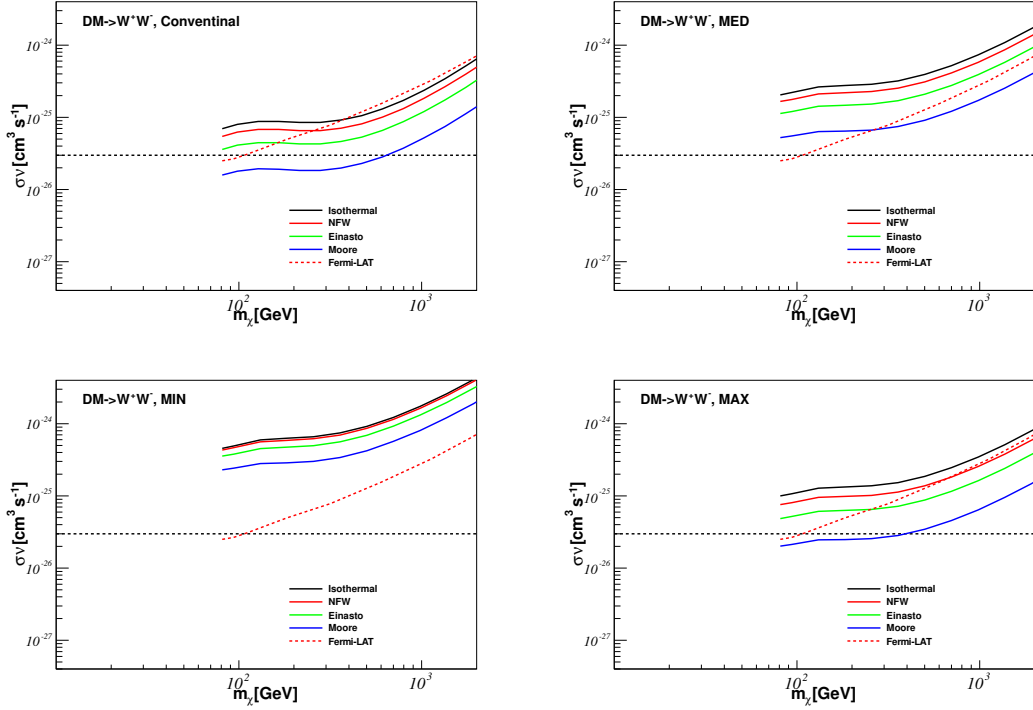


FIG. 4: The same as Fig. 3, but for DM annihilation into W^+W^- final states.

the variation of the upper limits is within about a factor of five.

For the W^+W^- final states, the results are shown in Fig. 4. The constraints from AMS-02 \bar{p}/p data turn out to be more stringent than that from the Fermi-LAT gamma-ray data for all the four DM profiles in the “convention” model when the DM particle mass is above ~ 300 GeV. Again we find that the variation of the upper limits from the “MIN” to the “MAX” model is within a factor of five. The result for the $q\bar{q}$ final states is shown in Fig. 5. Similar to the case of W^+W^- final states, the constraints from \bar{p}/p data are more stringent at about ~ 300 GeV. Compared with the case of W^+W^- and $b\bar{b}$, the constraints on the $q\bar{q}$ final states are the most stringent. For all the three final states, we find that the allowed DM annihilation cross section is below the typical thermal cross section for $m_\chi \lesssim 300$ GeV in the conventional propagation model with Einasto profile, which shows that the AMS-02 \bar{p}/p data can impose stringent constraints on DM candidates of weakly interacting massive particles.

As can be seen from Fig. 2, compared with the AMS-02 data the GALPROP DR models predict fewer antiprotons at low ($\lesssim 10$ GeV) and very high ($\gtrsim 100$ GeV) energies. Without a robust estimation of the theoretical uncertainties, it is premature to claim any excesses in the \bar{p}/p data. Nevertheless, we consider what would be the implications for DM if such a trend in the observations is confirmed by future analyses. The low energy

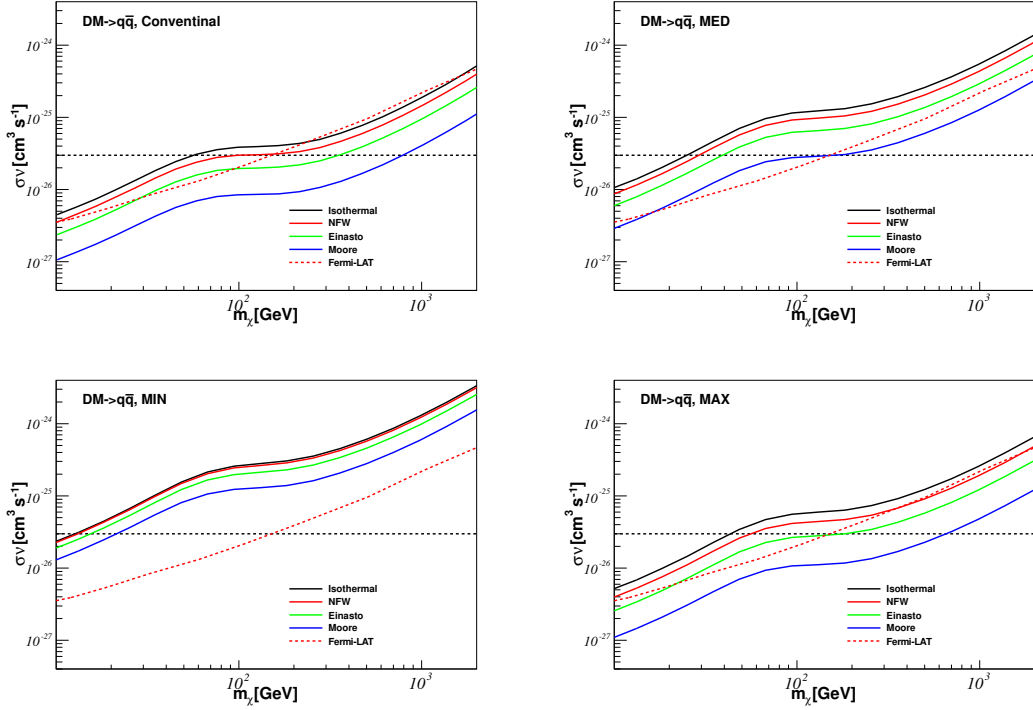


FIG. 5: The same as Fig. 3, but for DM annihilation into $q\bar{q}$ final states.

data would allow for a non-vanishing DM annihilation cross section. For instance, in the “conventional” propagation model, for $m_\chi = 10.1, 35.0$ and 75.8 GeV, the best-fit values are $\langle\sigma v\rangle = 3.6 \times 10^{-27}, 1.14 \times 10^{-26}$, and 2.79×10^{-26} cm^3s^{-1} , respectively, if the DM profile is Einasto, and the DM particles annihilate dominantly into $b\bar{b}$ final states. If both m_χ and $\langle\sigma v\rangle$ are allowed to vary freely, the best-fit DM particle masses and annihilation cross sections are

$$m_\chi = 58.5 \text{ (35.0) GeV and } \langle\sigma v\rangle = 2.16 \text{ (0.86)} \times 10^{-26} \text{ cm}^3\text{s}^{-1}$$

for DM annihilating into $b\bar{b}$ ($q\bar{q}$) final states. In Fig. 6, we show the calculated spectra of \bar{p}/p flux ratio from the best-fit DM particle masses and cross sections. The figure shows that the low energy \bar{p}/p data are well reproduced by including such a DM contribution, except for the data point with kinetic energy below 1 GeV.

As shown in Fig. 2, the spectrum of the AMS-02 \bar{p}/p ratio tends to be flat toward high energies above ~ 100 GeV. This trend, if confirmed by the future AMS-02 data, is not expected from the secondary production of antiprotons, and raises the interesting question whether this would leave some room for a heavy DM contribution, similar to the case of the AMS-02 positron fraction [44, 45, 46, 47, 48]. To explore this possibility, we perform an other fit using the \bar{p}/p ratio data above 20 GeV (15 data points in total)

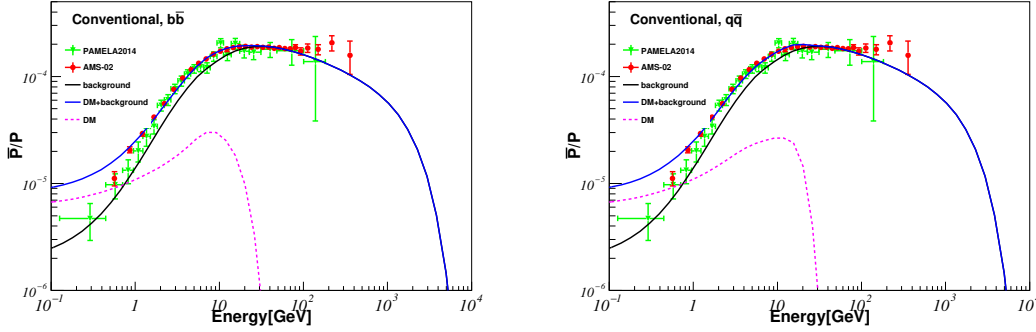


FIG. 6: Left) Spectrum of \bar{p}/p flux ratio from DM annihilating into $b\bar{b}$ final states with $m_\chi = 58.5$ GeV and $\langle\sigma v\rangle = 2.16 \times 10^{-26} \text{ cm}^3\text{s}^{-1}$ obtained from a fit to the whole AMS-02 \bar{p}/p data [2]. The “conventional” background model and the Einasto DM profile are assumed. Right) The same as left, but for the fit with $q\bar{q}$ final state with the best-fit values $m_\chi = 35$ GeV and $\langle\sigma v\rangle = 0.86 \times 10^{-26} \text{ cm}^3\text{s}^{-1}$.

in order to avoid the theoretical uncertainties in the low energy region. The obtained χ^2_{\min} as a function of m_χ for the $b\bar{b}$, $q\bar{q}$ and W^+W^- final states in the “conventional” propagation model with Einasto DM profile are shown in Fig. 7. One can see that for the three final states the values of χ^2_{\min} decrease almost monotonically from ~ 21 to ~ 5 with an increasing DM particles mass from 100 GeV to 10 TeV, but the χ^2 -curves become gradually flat toward high DM masses. Only for the W^+W^- channel, there exists a shallow local minimal at around 6.5 TeV with low statistical significance. From the χ^2 -curves, one can see that the DM particles mass is restricted to be above ~ 2 TeV at 2σ . For an illustration purpose, we show in Fig. 7 the predictions for the \bar{p}/p ratio in the “conventional” background model with a DM contribution. The DM particles masses and annihilation cross sections chosen to be $m_\chi = 6.5$ TeV, $\langle\sigma v\rangle = 1.9 \times 10^{-24} \text{ cm}^3\text{s}^{-1}$ for W^+W^- , $m_\chi = 10.9$ TeV, $\langle\sigma v\rangle = 3.4 \times 10^{-24} \text{ cm}^3\text{s}^{-1}$ for $b\bar{b}$ channel, and $m_\chi = 10.9$ TeV and $\langle\sigma v\rangle = 3.3 \times 10^{-24} \text{ cm}^3\text{s}^{-1}$ for $q\bar{q}$ channel. Note that these values are not from the best-fit values. We conclude that introducing a DM contribution can improve the agreement with the AMS-02 \bar{p}/p data with kinetic energy above 100 GeV, but the statistics is not high enough to determine the DM properties such as its mass and interaction strength. If the DM particle mass is indeed at $\mathcal{O}(10)$ TeV scale, next generation precision cosmic-ray detection experiments are needed. As can be see in Fig. 2, the possible “excess” is located at the kinetic energy range 100 – 450 GeV where the secondary backgrounds from the four propagation models are similar. However, beyond ~ 450 GeV, the \bar{p}/p from the “conventional” model drops quicker than that in the other propagation models. The future high energy antiproton data will be very important not only in probing DM but also in

constraining the background models.

In summary, we have explored the significance of the first AMS-02 \bar{p}/p data on constraining the annihilation cross sections of the DM particles in various propagation models and DM profiles. Four representative background models have been considered with four different DM profiles. We have derived the upper limits using the GALPROP code and shown that in the “conventional ” propagation model with Einasto DM profile, the constraints can be more stringent than that derived from the Fermi-LAT gamma-ray data on the dwarf spheroidal satellite galaxies. Making use of the typical minimal, median and maximal models obtained from a previous global fit, we have shown that the uncertainties on the upper limits is around a factor of five. The future more precise AMS-02 data can help to reduce the uncertainties in the derived upper limits.

Note added: As we were completing this study, Ref. [32] appeared on the arXiv, which addresses some of the same problems as discussed here. Although the conclusions are similar, the analysis in this work is based on the fully numerical GALPROP code, while that in [32] is based on the two-zone diffusion model with (semi)-analytical approach. The two methods are quite complementary to each other. Compared with Ref [32], the upper limits obtained in this work are weaker at DM particle mass below ~ 100 GeV, but stronger for heavy DM particles above ~ 500 GeV for typical DM particles annihilating into $\bar{b}b$ final states. Similar discussions on the DM matter contributions can be found in Refs. [49, 50].

Acknowledgments

YLW is grateful to S. Ting for warm hospitality and insightful discussions during his visit to the AMS-02 POCC at CERN. We thank P. Zuccon, A. Kounine, A. Oliva and S. Haino for helpful discussions on the details of the AMS-02 detector. This work is supported in part by the National Basic Research Program of China (973 Program) under Grants No. 2010CB833000; the National Nature Science Foundation of China (NSFC) under Grants No. 10905084, No. 11335012 and No. 11475237; The numerical calculations were done using the HPC Cluster of SKLTP/ITP-CAS.

References

- [1] **Planck** Collaboration, P. Ade et al., *Planck 2015 results. XIII. Cosmological parameters*, [arXiv:1502.01589](https://arxiv.org/abs/1502.01589).
- [2] S.Ting, talk at *AMS-02 days at CERN*, April 15-17, CERN, Geneva, <https://indico.cern.ch/event/381134/timetable/#20150415>.

- [3] D. Hooper, T. Linden, and P. Mertsch, *What Does The PAMELA Antiproton Spectrum Tell Us About Dark Matter?*, *JCAP* **1503** (2015), no. 03 021, [[arXiv:1410.1527](#)].
- [4] R. Kappl and M. W. Winkler, *The Cosmic Ray Antiproton Background for AMS-02*, *JCAP* **1409** (2014) 051, [[arXiv:1408.0299](#)].
- [5] N. Fornengo, L. Maccione, and A. Vittino, *Constraints on particle dark matter from cosmic-ray antiprotons*, *JCAP* **1404** (2014) 003, [[arXiv:1312.3579](#)].
- [6] M. Cirelli and G. Giesen, *Antiprotons from Dark Matter: Current constraints and future sensitivities*, *JCAP* **1304** (2013) 015, [[arXiv:1301.7079](#)].
- [7] H.-B. Jin, S. Miao, and Y.-F. Zhou, *Implications of the latest XENON100 and cosmic ray antiproton data for isospin violating dark matter*, *Phys.Rev.* **D87** (2013), no. 1 016012, [[arXiv:1207.4408](#)].
- [8] V. Ginzburg, V. Dogiel, V. Berezhinsky, S. Bulanov, and V. Ptuskin, *Astrophysics of cosmic rays*, .
- [9] A. Strong and I. Moskalenko, *Propagation of cosmic-ray nucleons in the galaxy*, *Astrophys.J.* **509** (1998) 212–228, [[astro-ph/9807150](#)].
- [10] L. Gleeson and W. Axford, *Solar Modulation of Galactic Cosmic Rays*, *Astrophys.J.* **154** (1968) 1011.
- [11] A. Strong and I. Moskalenko, *Propagation of cosmic-ray nucleons in the galaxy*, *Astrophys.J.* **509** (1998) 212–228, [[astro-ph/9807150](#)].
- [12] I. V. Moskalenko, A. W. Strong, J. F. Ormes, and M. S. Potgieter, *Secondary anti-protons and propagation of cosmic rays in the galaxy and heliosphere*, *Astrophys.J.* **565** (2002) 280–296, [[astro-ph/0106567](#)].
- [13] A. Strong and I. Moskalenko, *Models for galactic cosmic ray propagation*, *Adv.Space Res.* **27** (2001) 717–726, [[astro-ph/0101068](#)].
- [14] I. V. Moskalenko, A. Strong, S. Mashnik, and J. Ormes, *Challenging cosmic ray propagation with antiprotons. Evidence for a fresh nuclei component?*, *Astrophys.J.* **586** (2003) 1050–1066, [[astro-ph/0210480](#)].
- [15] V. Ptuskin, I. V. Moskalenko, F. Jones, A. Strong, and V. Zirakashvili, *Dissipation of magnetohydrodynamic waves on energetic particles: impact on interstellar turbulence and cosmic ray transport*, *Astrophys.J.* **642** (2006) 902–916, [[astro-ph/0510335](#)].

- [16] F. Donato, D. Maurin, P. Salati, A. Barrau, G. Boudoul, et al., *Anti-protons from spallations of cosmic rays on interstellar matter*, *Astrophys.J.* **563** (2001) 172–184, [[astro-ph/0103150](#)].
- [17] D. Maurin, R. Taillet, F. Donato, P. Salati, A. Barrau, et al., *Galactic cosmic ray nuclei as a tool for astroparticle physics*, [astro-ph/0212111](#).
- [18] F. Donato, N. Fornengo, D. Maurin, and P. Salati, *Antiprotons in cosmic rays from neutralino annihilation*, *Phys.Rev.* **D69** (2004) 063501, [[astro-ph/0306207](#)].
- [19] A. Putze, L. Derome, and D. Maurin, *A Markov Chain Monte Carlo technique to sample transport and source parameters of Galactic cosmic rays: II. Results for the diffusion model combining B/C and radioactive nuclei*, *Astron.Astrophys.* **516** (2010) A66, [[arXiv:1001.0551](#)].
- [20] M. Cirelli, G. Corcella, A. Hektor, G. Hutsi, M. Kadastik, et al., *PPPC 4 DM ID: A Poor Particle Physicist Cookbook for Dark Matter Indirect Detection*, *JCAP* **1103** (2011) 051, [[arXiv:1012.4515](#)].
- [21] O. Adriani, G. Barbarino, G. Bazilevskaya, R. Bellotti, M. Boezio, et al., *A new measurement of the antiproton-to-proton flux ratio up to 100 GeV in the cosmic radiation*, *Phys.Rev.Lett.* **102** (2009) 051101, [[arXiv:0810.4994](#)].
- [22] **PAMELA** Collaboration, O. Adriani et al., *PAMELA results on the cosmic-ray antiproton flux from 60 MeV to 180 GeV in kinetic energy*, *Phys.Rev.Lett.* **105** (2010) 121101, [[arXiv:1007.0821](#)].
- [23] **PAMELA** Collaboration, O. Adriani et al., *The cosmic-ray electron flux measured by the PAMELA experiment between 1 and 625 GeV*, *Phys.Rev.Lett.* **106** (2011) 201101, [[arXiv:1103.2880](#)].
- [24] **Fermi-LAT** Collaboration, M. Ackermann et al., *Fermi LAT observations of cosmic-ray electrons from 7 GeV to 1 TeV*, *Phys.Rev.* **D82** (2010) 092004, [[arXiv:1008.3999](#)].
- [25] **Fermi-LAT** Collaboration, *Fermi-LAT Observations of the Diffuse Gamma-Ray Emission: Implications for Cosmic Rays and the Interstellar Medium*, *Astrophys.J.* **750** (2012) 3, [[arXiv:1202.4039](#)].
- [26] H.-B. Jin, Y.-L. Wu, and Y.-F. Zhou, *Cosmic ray propagation and dark matter in light of the latest AMS-02 data*, [arXiv:1410.0171](#).

- [27] F. Donato, N. Fornengo, D. Maurin, and P. Salati, *Antiprotons in cosmic rays from neutralino annihilation*, *Phys.Rev.* **D69** (2004) 063501, [[astro-ph/0306207](#)].
- [28] **AMS** Collaboration, S. Haino, *Precision measurement of the proton flux with AMS, in talk at the 33rd international cosmic ray conference (ICRC2013), Rio de Janeiro, 2013*, 2013.
- [29] **AMS** Collaboration, A. Oliva, *Precision Measurement of the Cosmic Ray Boron-to-Carbon Ratio with AMS, in talk at the 33rd international cosmic ray conference (ICRC2013), Rio de Janeiro, 2013*, 2013.
- [30] I. V. Moskalenko, A. W. Strong, J. F. Ormes, and M. S. Potgieter, *Secondary anti-protons and propagation of cosmic rays in the galaxy and heliosphere*, *Astrophys.J.* **565** (2002) 280–296, [[astro-ph/0106567](#)].
- [31] I. V. Moskalenko, A. Strong, S. Mashnik, and J. Ormes, *Challenging cosmic ray propagation with antiprotons. Evidence for a fresh nuclei component?*, *Astrophys.J.* **586** (2003) 1050–1066, [[astro-ph/0210480](#)].
- [32] G. Giesen, M. Boudaud, Y. Genolini, V. Poulin, M. Cirelli, et al., *AMS-02 antiprotons, at last! Secondary astrophysical component and immediate implications for Dark Matter*, [arXiv:1504.04276](#).
- [33] O. Adriani, G. Barbarino, G. Bazilevskaya, R. Bellotti, M. Boezio, et al., *The PAMELA Mission: heralding a new era in precision cosmic ray physics*, *Phys.Rept.* **544** (2014) 323–370.
- [34] O. Adriani, G. Barbarino, G. Bazilevskaya, R. Bellotti, M. Boezio, et al., *Measurement of boron and carbon fluxes in cosmic rays with the PAMELA experiment*, *Astrophys.J.* **791** (2014) 93, [[arXiv:1407.1657](#)].
- [35] P. Salucci, F. Nesti, G. Gentile, and C. Martins, *The dark matter density at the Sun’s location*, *Astron.Astrophys.* **523** (2010) A83, [[arXiv:1003.3101](#)].
- [36] J. F. Navarro, C. S. Frenk, and S. D. White, *A Universal density profile from hierarchical clustering*, *Astrophys.J.* **490** (1997) 493–508, [[astro-ph/9611107](#)].
- [37] L. Bergstrom, P. Ullio, and J. H. Buckley, *Observability of gamma-rays from dark matter neutralino annihilations in the Milky Way halo*, *Astropart.Phys.* **9** (1998) 137–162, [[astro-ph/9712318](#)].

- [38] B. Moore, S. Ghigna, F. Governato, G. Lake, T. R. Quinn, et al., *Dark matter substructure within galactic halos*, *Astrophys.J.* **524** (1999) L19–L22, [[astro-ph/9907411](#)].
- [39] J. Diemand, B. Moore, and J. Stadel, *Convergence and scatter of cluster density profiles*, *Mon.Not.Roy.Astron.Soc.* **353** (2004) 624, [[astro-ph/0402267](#)].
- [40] J. Einasto, *Dark Matter*, [arXiv:0901.0632](#).
- [41] T. Sjostrand, S. Mrenna, and P. Z. Skands, *A Brief Introduction to PYTHIA 8.1*, *Comput.Phys.Commun.* **178** (2008) 852–867, [[arXiv:0710.3820](#)].
- [42] P. Ilten, *Tau Decays in Pythia 8*, *Nucl.Phys.Proc.Suppl.* **253-255** (2014) 77–80, [[arXiv:1211.6730](#)].
- [43] **Fermi-LAT** Collaboration, M. Ackermann et al., *Searching for Dark Matter Annihilation from Milky Way Dwarf Spheroidal Galaxies with Six Years of Fermi-LAT Data*, [arXiv:1503.02641](#).
- [44] **AMS** Collaboration, L. Accardo et al., *High Statistics Measurement of the Positron Fraction in Primary Cosmic Rays of 0.5C500 GeV with the Alpha Magnetic Spectrometer on the International Space Station*, *Phys.Rev.Lett.* **113** (2014) 121101.
- [45] J. Kopp, *Constraints on dark matter annihilation from AMS-02 results*, *Phys.Rev.* **D88** (2013) 076013, [[arXiv:1304.1184](#)].
- [46] L. Bergstrom, T. Bringmann, I. Cholis, D. Hooper, and C. Weniger, *New limits on dark matter annihilation from AMS cosmic ray positron data*, *Phys.Rev.Lett.* **111** (2013) 171101, [[arXiv:1306.3983](#)].
- [47] H.-B. Jin, Y.-L. Wu, and Y.-F. Zhou, *Implications of the first AMS-02 measurement for dark matter annihilation and decay*, *JCAP* **1311** (2013) 026, [[arXiv:1304.1997](#)].
- [48] Z.-P. Liu, Y.-L. Wu, and Y.-F. Zhou, *Sommerfeld enhancements with vector, scalar and pseudoscalar force-carriers*, *Phys.Rev.* **D88** (2013) 096008, [[arXiv:1305.5438](#)].
- [49] M. Ibe, S. Matsumoto, S. Shirai, and T. T. Yanagida, *Wino Dark Matter in light of the AMS-02 2015 Data*, *Phys. Rev.* **D91** (2015), no. 11 111701, [[arXiv:1504.05554](#)].
- [50] C.-H. Chen, C.-W. Chiang, and T. Nomura, *Dark matter for excess of AMS-02 positrons and antiprotons*, *Phys. Lett.* **B747** (2015) 495–499, [[arXiv:1504.07848](#)].

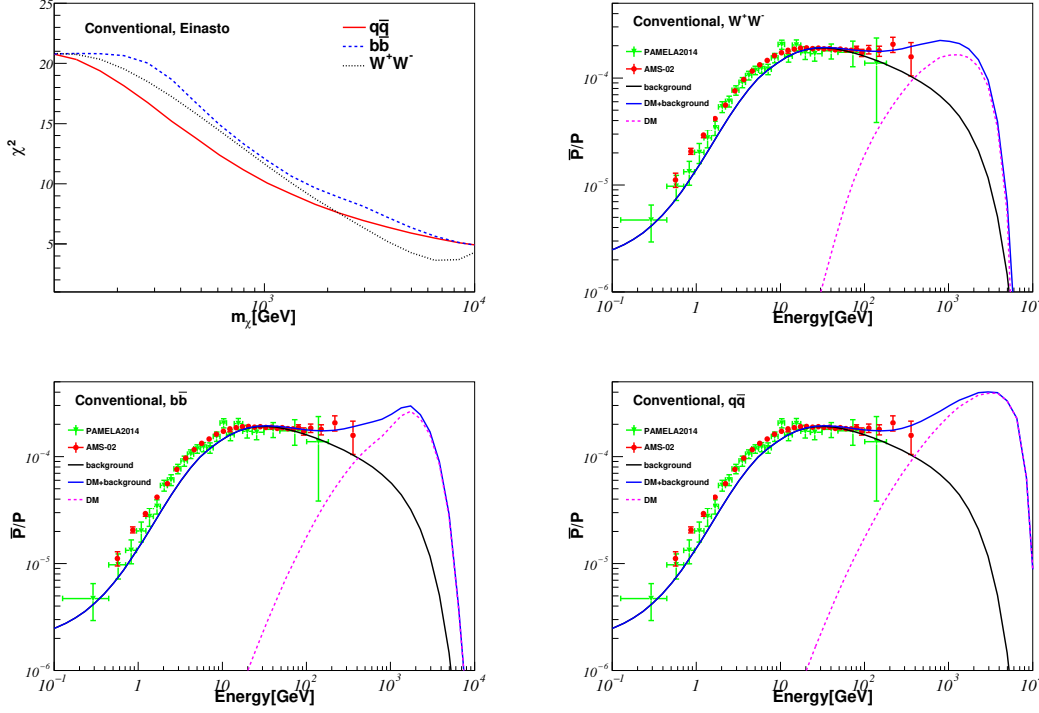


FIG. 7: (Upper left) values of χ^2_{\min} as a function of DM particle mass m_χ from a fit to the AMS-02 \bar{p}/p data (with kinetic energy above 20 GeV) in the “conventional” propagation model [13, 15] with the DM profile fixed to Einasto [40]. Three annihilation channels $b\bar{b}$, $q\bar{q}$ and W^+W^- are considered. (Upper right) predicted \bar{p}/p ratio in the case of background (“conventional” model) plus a DM contribution with $m_\chi = 6.5$ TeV, $\langle\sigma v\rangle = 1.9 \times 10^{-24} \text{cm}^3 \text{s}^{-1}$, and annihilation final states W^+W^- . The flux ratio of antiproton from DM to the proton from the background $\bar{p}_{\text{DM}}/p_{\text{BG}}$ is shown as the dashed line. The data from AMS-02 [2] and PAMELA [33] are also shown. (Lower left) the same as the upper right, but for the $b\bar{b}$ channel with $m_\chi = 10.9$ TeV and $\langle\sigma v\rangle = 3.4 \times 10^{-24} \text{cm}^3 \text{s}^{-1}$. (Lower right) the same as the upper right, but for the $q\bar{q}$ channel with $m_\chi = 10.9$ TeV and $\langle\sigma v\rangle = 3.3 \times 10^{-24} \text{cm}^3 \text{s}^{-1}$.